RSC Advances

Cite this: DOI: 10.1039/c0xx00000x

www.rsc.org/xxxxxx

ARTICLE TYPE

An Attempt to fabricate Photocatalytic and Hydrophobic Self-cleaning Coating via Electrospinning

Prathapan Ragesh,[a] Shantikumar V Nair[a] and A. Sreekumaran Nair*[a]

Received (in XXX, XXX) XthXXXXXXXXX 20XX, Accepted Xth XXXXXXXXX 20XX
DOI: 10.1039/b000000x

Fluorinated POSS (Polyhedral oligomeric silsesquioxanes) was blended with PVDF (poly (vinylidene fluoride)/TiO_2 (titanium dioxide) composite by stirring for overnight and the resultant solution was electrospun to obtain POSS/PVDF/TiO_2 micron- and nanofibers with self-cleaning capacity. The coatings were deposited on a fluorosilane-treated glass substrate and it showed both hydrophobicity and photocatalytic activity. The morphology of the fabricated coating was analysed using scanning electron microscopy and atomic force microscopy. The optical property of the coating was studied using UV-visible spectroscopy, which gave around 65-70% transmittance with just 2% of POSS inclusion. Membrane stability on the substrate was checked with nano-scratch test. The Nano-scratch test indicates that the tip of the nano-indenter was unable to percolate through the membrane; rather it just ploughs around its surface, revealing the adhesion of coatings and mechanical stability. The Contact angle measurements showed a value of 135.5° for the F-POSS/PVDF/TiO_2 coating, thus showing its hydrophobic nature. The photocatalytic effect of the membrane was checked with respect to the degradation of methyl orange dye under UV exposure. The surface roughness calculated from the AFM measurements showed that the inclusion of POSS into the nanofibers enhanced the surface roughness. We anticipate that the thermally and mechanically stable coating may find immense applications in many real areas like water-purification, window panels, glass modules for photovoltaic devices, etc.

Introduction

Self-Cleaning coatings, a remarkable idea of biomimicing the Nature finds immense applications[1-9] in corrosion resistance, oil repellence, anti-icing, anti-bacterial, window panels, water-purification, glass modules for solar panels, textiles etc. Several effects are designed from the natural complexity present in wings of butterflies,[10] lotus leaf,[11,12] water strider legs,[13]cicada wings,[14] gecko feet,[15] etc. Generally, the self-cleaning coatings are categorized into super-hydrophilic[16-20] and super-hydrophobic[21-31]. The former shows a cleansing action by the rolling of water droplets that carries away the dirt particles, while the latter clean surfaces by the photocatalytic degradation[32-36] process and sheeting of water. The wettability of the coating depends upon the surface roughness and surface energy.[37,38] Many polymers are available in Nature that are hydrophobic, which after surface modification changes into superhydrophobic materials. Among them fluorinated polymers are of great interest because of their inherent superhydrophobicity owing to low surface energy and high roughness.[39-42] POSS (Polyhedral Oligomeric Silsesquioxane) has a general structure of $[RSi]_n[O1.5]_n$ where R represents the organic substituents and Si and O refers to silicon and oxygen groups. The R group imparts the organic behaviour whereas O-Si linkages impart the inorganic character to the POSS. Different structure of Silsesquioxane can be seen such as ladder, random, cage or partial cage structures,[43,44] among which the cage structure is of great interest. The presence of silica cages make them thermally stable. The organic groups present on the external cage structure make them miscible or compatible with many organic solvents/polymers thereby facilitating functionality.[45] Several POSS-polymer blends can be synthesized which have salient characteristics like high mechanical resistance, enhanced glass-transition temperature, high mechanical strength etc., that make them a potential candidate in various fields like biological, aerospace, electronics applications, etc.[46-50] Even though several synthesizing techniques are available for fabricating self-cleaning coatings such as spin-coating,[51] spray deposition,[52] dip-coating,[53] etc., they face limitations like difficulty in controlling the thickness of the coating deposited. Electrospinning technique is a versatile technique which can be used to fabricate continuous polymeric nanofibers[54-57] with controlled orientation of fibers[58-60] and enhanced roughness.[61]

Various coatings with hydrophobic materials have been reported in plenty, but the coatings showing both hydrophobic and photocatalytic behavior are rarely there. In this work, we made an attempt to fabricate '**a hydrophobic and photocatalytic coating**' using the F-POSS/PVDF/TiO_2 composite. Electrospinning the above materials' combination on a substrate resulted in a coating (consisting of beaded fibers) with enhanced roughness. The thickness of the coating has been optimized for transparency and the coating has been characterized for its

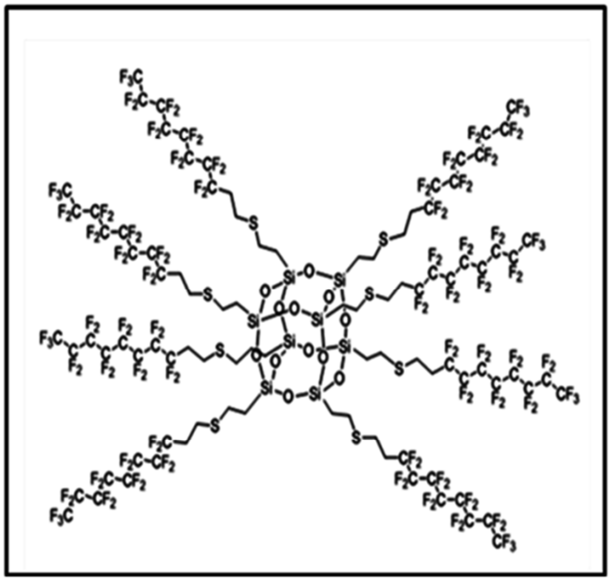

Fig. 1. Chemical structure of F-POSS (FP8).[23]

wettability, thermal and mechanical stability, roughness and morphology, etc.

Materials and Methods

(a) Materials

Titanium (IV) isopropoxide (TiP, 99.99%, Aldrich, USA), Poly (vinylidene fluoride) (PVDF, Average Mw~ 534,000 by GPC powder) was purchased from Sigma Aldrich, USA. *N,N*-dimethylformamide (anhydrous, 99.8%), methanol (99.8%) and tetrahydrofuran (THF, anhydrous, ~ 99.9%, inhibitor free) were purchased from Sigma Aldrich, Germany. Fluorinated polyhedral oligomeric silsesquioxanes (F-POSS, FP8) was gifted by IMRE, Singapore. (Tridecafluoro-1,1,2,2-tetrahydrooctyl)-1-trichlorosilane was from Alfa Aesar, UK (97%). Glycerol (98% purified) and ethylene glycol (for synthesis grade) were purchased from MERCK, Germany. Titanium dioxide (TiO_2 P25, AeroxideR) was purchased from Degussa, Germany. Microsope slides (26 x 76mm, 1mm-1.2mm thick) were purchased from Labtech Medico (P) Ltd. Scotch tape was a product of Magic tape with 12 mm x 4m). Isopropyl alcohol (99%), methyl Orange powder (indicators) and Malachite Green (fast green/light green) were purchased from Nice Chemicals, India.

(b) Solution and substrate preparation

A series of cleaning process were done to make the glass slides clean else will affect the transparency once the coating is deposited. The glass slides were cleaned by ultrasonicating them in deionized water, soap solution, isopropyl alcohol and methanol, each for approximately 15 minutes, respectively. The cleaned glasses were then dried using the oven for about 1 h at 60 °C. The dried glass slides were treated with 30 µL of fluorosilane to improve the adhesion between the glass substrates and the F-POSS. before electrospinning About 1.1 g PVDF was taken in a Borosil beaker and was dissolved in a mixture of 5 mL DMF and

(c) Electrospinning

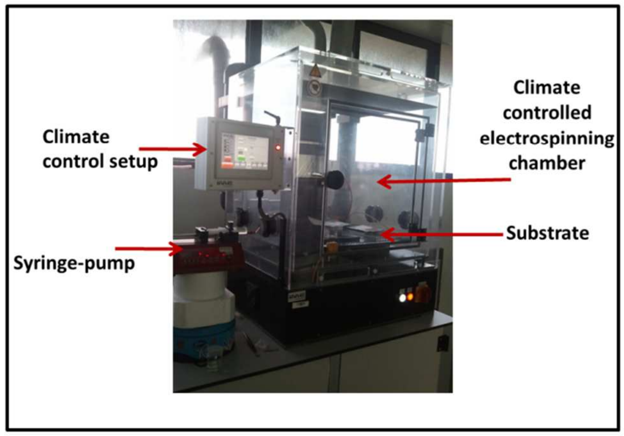

Fig. 2. Front view of the electrospinning set-up used.

5mL THF. Into the above solution, 2 wt.% F-POSS (22 mg) and 1 wt.% TiO_2 (11 mg) were added and the resultant solution was stirred overnight. While stirring overnight, the Borosil beaker was covered with a parafilm so as to avoid the entry of any moisture. The structure of POSS (FP8) used is given in **Fig. 1**. The above composition is an optimized one after a series of tests on spinnability. The resultant POSS/PVDF/TiO_2 solution was poured into a 10 mL syringe and was then loaded into electrospinning machine (IME Technologies, The Netherlands). A static collector was used to collect the random fibers on the cleaned glasses mounted on it. A voltage of 25 kV was applied at the tip of the needle syringe with a flow rate of 0.1 mL/h. Temperature and humidity of the chamber were set to ~ 25 °C and ~ 50%, respectively. The distance between the needle-tip (26G ½) and the collector was set to 15cm. The electrospinning of the precursor solution was done for 1-2 min to obtain a transparent coating on the glass substrate, which was then warmed at 60 °C for 30 min so as to remove the solvent residues. The electrospinning setup is shown in **Fig. 2**. The fibres on the glass substrate were then stored in a well-maintained desiccator to avoid any contamination. Also the fibers were deposited thickly on aluminium (Al) foil for more than 4 h so that we can take out the film from the Al foil and analyse for various characterizations like Nanoidendation study, photocatalysis study, etc.

Instrumentation and Characterization

Morphology of the fibre samples were obtained using Scanning Electron Microscopy (SEM) (JEOL JSM 6490 LA). Sample preparation for SEM involved sputtering of a gold layer on the as-spun POSS/PVDF/TiO_2 fibres so as to make it conductive. For the identification of the components in the fabricated coating, energy dispersive X-ray spectroscopy (EDS, FEI Quanta 200) was carried out. Using a surface Profilometer (Veeco, Dektak 150), the thickness of the coating was measured. Atomic Force Microscopy (AFM, JEOL SPM 5200) measurements were done to evaluate the roughness and topology of the fabricated coating. The optical properties of the coating were analysed using a UV-VIS-NIR Spectrometer (PerkinElmer, Lambda 750). Wettability

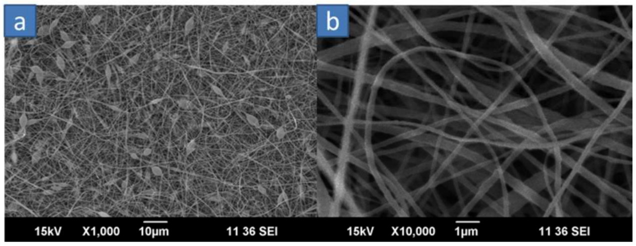

Fig. 3 (a and b) High and low magnification SEM images of the as-spun POSS/PVDF/TiO_2 coating

property of the coating was analysed using a contact angle measuring set-up (Digidrop MCAT, France). To check the mechanical stability of the coating with the glass substrate, Scratch test was carried out using a Nanoindentation set-up (Hysitron Tribo Indenter 950. The photocatalytic activity of the TiO_2 in the POSS/PVDF/TiO_2 coating was confirmed by performing the photocatalytic degradation of methyl orange under ultraviolet radiation at different time intervals.

Results and discussion

The surface morphology of the as-spun POSS/PVDF/TiO_2 coating can be seen in **Fig. (3a and 3b)**, respectively. It is observed that the as-fabricated coating consists of a combination of nanofibers interfaced with micro fibers, where the latter was lower in number compared to the former. The fibres have an average diameter of 267 nm with 1 wt.% and 2 wt.% inclusion of TiO_2 and POSS, respectively. Such a higher fiber diameter is affected by factors like concentration,[62,63] viscosity and surface tension of the precursors in the solution used for electrospinning. The as-spun fibers had beaded structures. Nevertheless beaded fibers for self-cleaning applications have been reported earlier[64-67]. The presence of the constituent elements comprising the coating was confirmed using EDS measurement as seen in **Fig. 4**. Similarly the presence of POSS was confirmed with the presence of S, Si, O, C and F in the coating. To analyze the roughness and topology of the coating material, AFM measurements were done for 10 μm^2 area. Comparing the roughness of the control sample (without POSS), the POSS/PVDF/TiO_2 sample had more roughness as seen in Table 1, which may be attributed by the inclusion of POSS into the coating material. Also the samples had sufficient roughness due to the electrospinning technique. The topology of the POSS/PVDF/TiO_2 sample and the control sample can be seen from **Fig. 5**.

The wettability of the coating was tested using the contact angle measurement. 3 μL drop of DI water was made to contact the surface using a static mode of contact angle measurement. The triangular curve was drawn at the periphery of the water droplet sitting on the sample surface so as to get the equilibrium angle at the three phases - the liquid, vapour and the solid. Several trials were carried out in different parts of the POSS/PVDF/TiO_2 surface as well as for the control sample (without POSS) and the average contact angle was calculated out of five measurements. An average water contact angle of 135.5° and 129.40° was recorded for the sample with and without POSS, respectively. The increment in water contact angle is due to the inclusion of POSS in the coating which lowered the surface

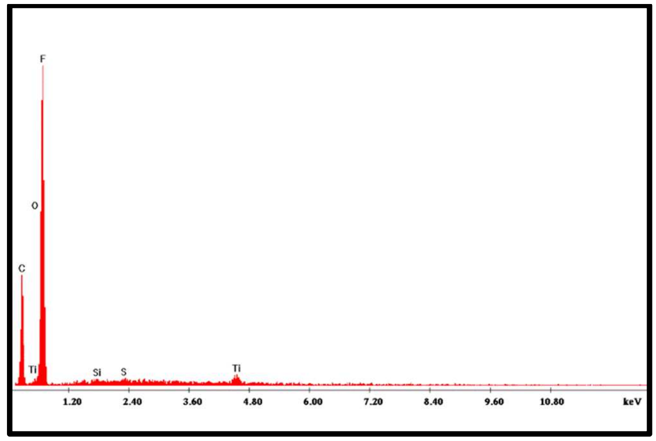

Fig.4 EDS spectra of POSS/PVDF/TiO_2 with 1 wt. % TiO_2 and 2 wt.% POSS added to 1.1g of PVDF sample.

energy and enhanced the roughness of the material. Ganesh et al.[23] has already proven that inclusion of fluorinated POSS in the coating material enhances the Water contact angle. But here only a slight increment is observed as we have added only just 2wt.% of POSS into the coating material. The optical image of the sessile water drop for contact angle measurement can be seen in **Fig. 6**.

To check whether the surface is photocatalytic in nature, degradation of methyl orange dye under ultraviolet radiation was done. The presence of TiO_2 makes the surface photocatalytic in

Table 1. Roughness parameters obtained from AFM measurement.

Sample	*R_a (μm)*	*R_q (μm)*	*R_z (μm)*
POSS/PVDF/TiO_2	0.720	0.841	4.51
PVDF/TiO_2 (Control)	0.446	0.548	3.39

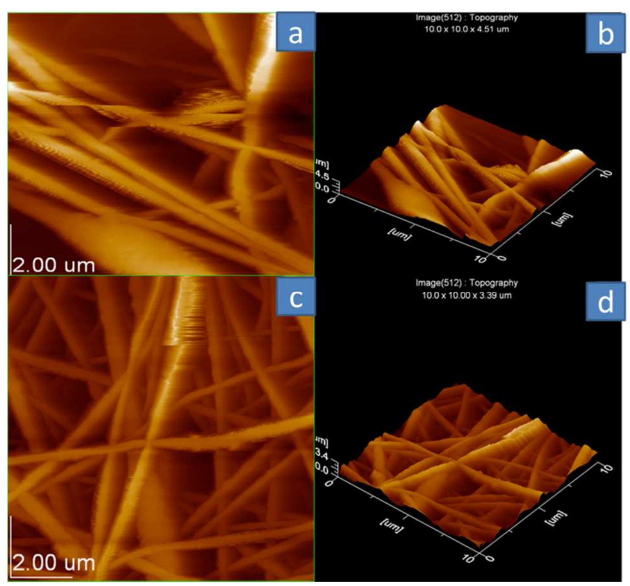

Fig. 5 (a and b) 2-D and 3-D AFM image of the POSS/PVDF/TiO_2 coating sample, (c and d) 2-D and 3-D AFM image of the PVDF/TiO_2 (control) sample. For both the samples the AFM analysis was done for an area of 10 μm^2.

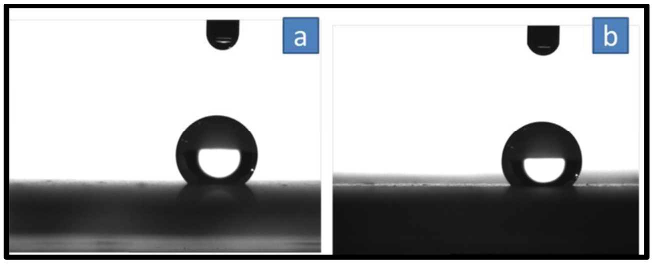

Fig.6 (a and b). The optical image taken while the water drop comes into contact to the surface with POSS and without POSS, respectively.

nature. POSS/PVDF/TiO_2 coating deposited on the aluminium foil was taken and kept on a neat tissue paper on one side and on the other side, the coating of the control sample (without TiO_2) deposited on aluminium foil was taken out and just placed in a glass slide. The latter was done as the coating was lighter compared to the former, because of which it required any support while keeping in a plane surface. Both the coating material taken for the photocatalysis was of the same thickness. 1 mM solution of methyl orange dye in water was prepared and using the micropipette, a drop of the solution was kept on both the surfaces (surface with and without TiO_2). As both the surfaces had PVDF, the liquid drop was seen in a spherical shape. UV illumination was done on both the surfaces at a series of interval time (15 min, 30 min, 40 min, 50 min and 55 min) and for each speculated time, the photograph was taken as seen in **Fig. 7**. It was seen that by gradual exposure of the sample with TiO_2 to the ultraviolet radiation, the dye was decomposed by TiO_2 and nearly disappeared after 55 min. In the last photograph as seen in **Fig. 7e**, there was only a scar left behind. The reason is that the dye was added beyond the adsorption limit of the coating surface and also only 1 wt.% of TiO_2 was present in the coating to degrade the dye.

To check the membrane stability and the adhesiveness of the fabricated coating with the glass substrate, Nano-scratch test with 30 mN ramp load scratch using Hysitron Nano indenter was performed. A thicker film of 3.5 μm was deposited on the glass substrate to check the adhesiveness on a large scale. The scratch test was done at four different locations on each of the sample. High load transducer head equipped with conospherical probe was used for the experiment. The scratch length was 25 μm. It was observed that even though a higher ramping load of 30 mN was applied using the conospherical probe, the probe was unable to percolate through the coating. This is because the coating deposited was highly mechanically stable that it resisted any kind of foreign force to enter into the surface. As a result, the probe was just ploughing on the coating surface. Plots of Lateral force versus Normal force as seen in **Fig. 8b** was plotted and compared for both the surfaces with and without POSS. It was observed that

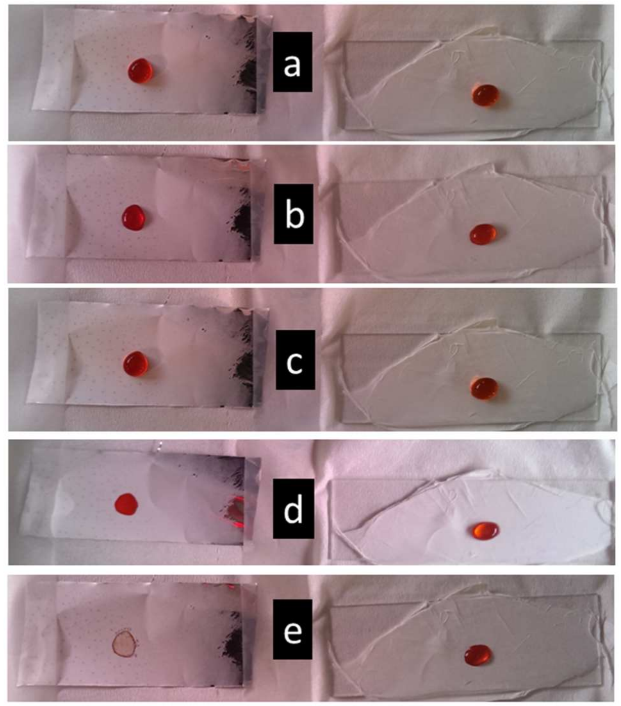

Fig. 7 The photographs showing the status of the methyl orange dye on the surfaces with (left column) and without TiO_2 (right column) upon ultraviolet illumination for a) 15 min, b) 30 min, c) 40 min, d) 50 min and e) 55 min.

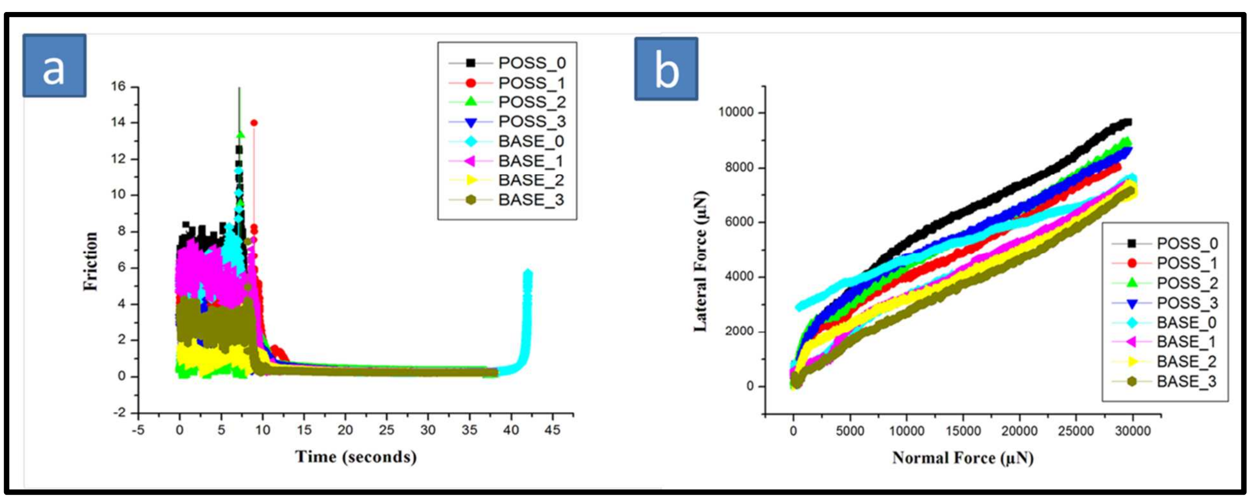

Fig. 8 a) Friction Profile of samples with and without POSS, being compared, b) The plot of lateral force versus normal force for samples with and without POSS which is being compared. In the figure, BASE indicates the control sample PVDF/TiO_2 (without POSS) and POSS indicates the main sample (POSS/PVDF/TiO_2). For both the plots (a and b), the scratch test was performed on four different sample locations.

Cite this: DOI: 10.1039/c0xx00000x

www.rsc.org/xxxxxx

ARTICLE TYPE

there was no delamination point even though a higher force of 30 mN ramp load was applied. Also a higher force resisting capacity was seen for POSS/PVDF/TiO_2 surfaces compared to the PVDF/TiO_2 surfaces. This is because of the fact that inclusion of POSS enhances the mechanical resistance. Also the plots of friction versus time was plotted and compared for both the samples (**Fig. 8a**) (with and without POSS). It was seen that there was no distinct changes in the friction profile as no delamination occurred even after applying a higher ramp load of 30 mN. In the **Fig. 8** (a and b), base indicates the control sample (PVDF/TiO_2) and POSS indicate the main sample (POSS/PVDF/TiO_2). The scratch test was performed on four different sample locations. We believe that fluorinated silane pre-treatment of the glass substrate might have helped in the firm attachment of the POSS/PVDF/TiO_2 composite coating on the glass. However, we have also found previously that direct electrospinning of the polymers (POSS/PVDF) and metal oxides (TiO_2) on glass substrates can also create respective stable coatings on substrates.[23,68]

The optical property of the fabricated POSS/PVDF/TiO_2 coating on glass substrate was analysed using UV-VIS-NIR spectrometer which scanned over a wavelength from 400 nm to 1000 nm. The transmittance plot for the plane glass was compared with the glass containing POSS/PVDF/TiO_2 coating (**Fig. 9a**). The plane glass showed a transmittance value of ~90%, whereas the glass coated with POSS/PVDF/TiO_2 showed a transmittance value of nearly 70%. In the literature, it is been reported that inclusion of 15 wt.% of FP8 fluoroPOSS[23] into the coating surface gives a transmittance value of 86%. But in our work, we have just used 2 wt.% of POSS and obtained an appreciable result. The decrement pattern of transmittance was observed from 900 nm to 400 nm. Similar patterns have been observed in literature too.[69-71] The reason may be due to the high roughness of the material used in the coating which increases hydrophobicity and thus decreases transmittance. Also as TiO_2 is added into the coating material, there will be an absorption peak arising in the UV-band edge. This may be also a reason contributing to the decreasing transmittance pattern. Even though the obtained transmittance was considerably low, physically the transparency was not much affected as seen in Fig. 11b. The letters in the newspaper can be seen through the glass bearing the coating (POSS/PVDF/TiO_2). Also the hydrophobicity of the coating is shown with water, glycerol (orange in colour) and ethylene glycol (dark blue) droplets sitting on the coating surface with minimal contact.

Conclusions

In summary, we have attempted to fabricate a self-cleaning coating with hydrophobicity and photocatalytic property using POSS/PVDF/TiO_2 composite. The coating fabricated was thermally and mechanically stable and robust. The characterization techniques like nanoidendation test, AFM, SEM, EDS and UV-visible spectroscopy were carried out to check the coating' functionalities. The methylene orange dye degradation under ultraviolet radiation confirmed the photocatalytic property of the coating induced by TiO_2. The contact angle measurement was carried out to confirm the hydrophobic nature of the coating with a water contact angle of 135.5°. Multifunctional coatings are a new area which can be explored extensively for applications such as for solar glass modules (self-cleaning and anti-reflective), anti-corrosion, anti-icing, etc.

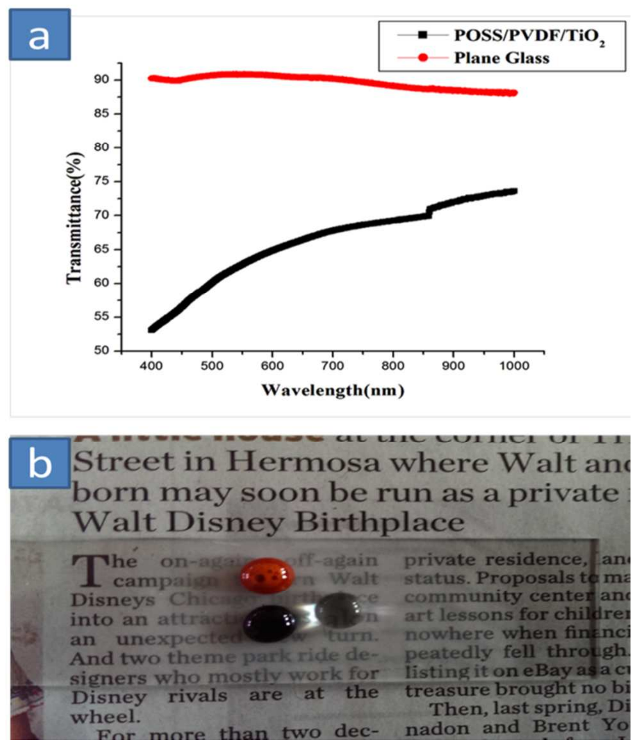

Fig. 9 a) Comparison of Transmittance plot for plane glass and glass with POSS/PVDF/TiO_2 coating, b) The transmittance of the glass bearing the POSS/PVDF/TiO_2 coating illustrated by placing the coated glass on a newspaper. The hydrophobic nature of the coating also seen through the droplets of water (colourless), glycerol (orange colour due to methylene orange dye) and ethylene glycol (darkish blue due to the addition of malachite green dye) which sits on the coating surface with minimal contact.

Acknowledgement

We acknowledge the Ministry of New and Renewable Energy, (MNRE), Govt. of India for the financial support for the project. We acknowledge INUP (Indian Institute of Technology, Mumbai), SAIF (Cochin) and Hysitron Company (Trivandrum, Kerala) for rendering their services for some of the characterization techniques. We also acknowledge Mr. Sajin. P, Ms. Anjusree G. S, Mr. Deepak T. G and Ms. Ragima Nadesh for their technical support. We also thank Mr. A. G. Venkatesan (of

National University of Singapore) and Dr. J. Xu (of IMRE, Singapore) for gifting us the POSS material.

Notes and references

[a]*Amrita Centre for Nanoscience & Molecular Medicine, Amrita Institute of Medical Science, AIMS Ponekkara PO, Kochi 682041, Kerala, India Email:sreekumarannair@aims.amrita.edu*

1 V. A. Ganesh, H. K. Raut, A. S. Nair and S. Ramakrishna, *J. Mater. Chem.*, 2011, **21**, 16304–16322.
2 Z. Guo, W. Liu and B. L. Su, *J. Colloid Interface Sci.*, 2011, **353**, 335–355.
3 L. Cao, T. P. Price, M. Weiss and D. Gao, *Langmuir*, 2008, **24**, 1640-1643.
4 A. Vilcnik, I. Jerman, A.Surca Vuk, M. Kozelj, B. Orel, B. Tomsic, B. Simoncic and J. Kovac, *Langmuir*, 2009, **25**, 5869-5880.
5 S. S. Chhatre, A. Tuteja, W. Choi, A. Revaux, D. Smith, J. M. Mabry, G. H. McKinley and R. E. Cohen, *Langmuir*, 2009, **25**, 13625-13632.
6 W. Choi, A. Tuteja, S. Chhatre, J. M. Mabry, R. E. Cohen and G. H. McKinley, *Adv. Mater.*, 2009, **21**, 2190-2195.
7 R. Misra, R. D. Cook and S. E. Morgan, *J. Appl. Polym. Sci.*, 2010, **115**, 2322-2331.
8 P. Muthiah, S. H. Hsu and W. Sigmund, *Langmuir*, 2010, **26**, 12483-12487.
9 Y. Y. Yan, N. Gao and W. Barthlott, *Adv. Colloid Interface Sci.*, 2011, **169**, 80-105.
10 D. Byun, J. Hong, Saputra, J. H. Ko, Y. J. Lee, H. C. Park, B. K. Byun and J. R. Luker, *J. Bionic Eng.*, 2009, **6**, 63-70.
11 Z. Z. Luo, Z. Z. Zhang, L. T. Hu, W. M. Liu, Z. G. Guo, H. J. Zhang and W. J. Wang, *Adv. Mater.*, 2008, **20**, 970-974.
12 A. Otten and S. Herminghaus, *Langmuir*, 2004, **20**, 2405-2408.
13 X. Gao, and L. Jiang, *Nature*, 2004, **432**, 36−36.
14 G. Zhang, J. Zhang, G. Xie, Z. Liu, H. Shao, *Small*, 2006, **2**, 1440−1443.
15 H. Lee, B. P. Lee, and P. B. Messersmith, *Nature*, 2007, **448**, 338−341.
16 S. Nishimoto, A. Kubo, X. Zhang, Z. Liu, N. Taneichi, T. Okui, T. Murakami, T. Komine, and A. Fujishima, *Appl. Surf. Sci.*, 2008, **254**, 5891−5894.
17 K.-i. Katsumata, C. E. J. Cordonier, T. Shichi, and A. Fujishima, *Mater. Sci. Eng., B*, 2010, **173**, 267-270.
18 K. Nakata, K. Udagawa, T. Ochiai, H. Sakai, T. Murakami, M. Abe, and A. Fujishima, *Mater. Chem. Phys.*, 2011, **126**, 484-487.
19 A. Fujishima, T. N. Rao, D. A. Tryk, *J. Photochem. Photobiol., C*, 2000, **1**, 1-21.
20 I. P. Parkin, and R. G. Palgrave, *J. Mater.Chem.*, 2005, **15**, 1689−1695.
21 X. Wang, B. Ding, J. Yu, and M. Wang, *Nano Today*, 2011, **6**, 510−530.
22 P. A. Levkin, F. Svec, and J. M. J. Fréchet, *Adv. Funct. Mater.*, 2009, **19**, 1993- 1998.
23 V. A. Ganesh, A. S. Nair, H. K. Raut, T. T. Y. Tan, C. He, S. Ramakrishna, and J. Xu, *J. Mater.Chem.*, 2012, **22**, 18479−18485.
24 Y.-L. Zhang, H. Xia, E. Kim, H.-B. Sun, *Soft Matter.*, 2012, **8**, 11217-11231.
25 M. Qu, B. Zhang, S. Song, L. Chen, J. Zhang, and X. Cao, *Adv. Funct. Mater.*, 2007, **17**, 593−596.
26 D. Wang, Z. Guo, Y. Chen, J. Hao, and W. Liu, *Inorg. Chem.*, 2007, **46**, 7707−7709.
27 L. Zou, X. Xiang, J. Fan, and F. Li, *Chem.Mater.*, 2007, **19**, 6518−6527.
28 C. W. Dunnill, K. Page, Z. A. Aiken, S. Noimark, G. Hyett, A. Kafizas, J. Pratten, M. Wilson, and I. P. Parkin, *J. Photochem. Photobiol. A*, 2011, **220**, 113-123.
29 H. Liu, S. Szunerits, M. Pisarek, W. Xu, and R. Boukherroub, *ACS Appl. Mater. Interfaces*, 2009, **1**, 2086-2091.
30 J. Zhang, G. Pu, S. J. Severtson, *ACS Appl. Mater. Interfaces,* 2010, **2**, 2880-2883.
31 D. Kitagawa and S. Kobatake, *Chem. Sci.*, 2012, **3**, 1445-1449.
32 S. Nishimoto, A. Kubo, K. Nohara, X. Zhang, N. Taneichi, T. Okui, Z. Liu, K. Nakata, H. Sakai, T. Murakami, M. Abe, T. Komine, and A. Fujishima, *Appl. Surf. Sci.*, 2009, **255**, 6221-6225.
33 Y. Li, T. Sasaki, Y. Shimizu, and N. Koshizaki, *Small*, 2008, **4**, 2286-2291.
34 Y. Li, T. Sasaki, Y. Shimizu, and N. Koshizaki, *J. Am. Chem. Soc.*, 2008, **130**, 14755-14762.
35 R. Prado, G. Beobide, A. Marcaide, J. Goikoetxea, and A. Aranzabe, *Sol. Energy Mater. Sol. Cells*, 2010, **94**, 1081-1088.
36 N. M. Bedford, and A. J. Steckl, *ACS Appl. Mater. Interfaces*, 2010, **2**, 2448−2455.
37 R. N. Wenzel, *Ind. Eng. Chem.*, 1936, **28**, 988-994.
38 A. B. D. Cassie and S. Baxter, *Trans. Faraday Soc.*, 1944, **40**, 546-551.
39 L. Feng, Z. Zhang, Z. Mai, Y. Ma, B. Liu, L. Jiang and D. Zhu, *Angew. Chem., Int. Ed.*, 2004, **43**, 2012.
40 J. Li, J. Fu, Y. Cong, Y. Wu, L. Xue and Y. Han, *Appl. Surf. Sci.*, 2006, **252**, 2229.
41 H. Y. Kwong, M. H. Wong, Y. W. Wong and K. H. Wong, *Appl. Surf. Sci.*, 2007, **253**, 8841-8845.
42 K. Wang, N. X. Hu, G. Xu and Y. Qi, *Carbon*, 2011, **49**, 1769-1774.
43 G. Li, L. Wang, H. Ni, and C. U. Pittman Jr, *J. Inorg Organomet Polym.*, 2001, **11**, 123–54.
44 G. Li C. U. Pittman Jr CU. Polyhedral oligomeric silsesquioxane (POSS) polymers, copolymers and resin nanocomposites. In: A. S. Abe-El-Aziz, C. E. Carraher Jr, C. U. Pittman Jr, and M. Zeldin, editors. Macromolecules containing metal and metal-like elements, vol. 4. Hoboken, NJ: John AWiley & Sons; 2005. p. 79-132.
45 S.-W. Kuo, F.-C. Chang, *Prog. Polym. Sci.*, 2011, **36**, 1649-1696.
46 G. Li, L. Wang, H. Ni and C. U. Pittman Jr., *J. Inorg. Organomet. Polym.*, 2001, **11**, 123-153.
47 S. H. Phillips, T. S. Haddad and S. J. Tomczak, *Curr. Opin. Colloid Interface Sci.*, 2004, **8**, 21-29.
48 K. Pielichowski, J. Njuguna, B. Janowski and J. Pielichowski, *Adv. Polym. Sci.*, 2006, **201**, 225-296.
50 J. Wu and P. T. Mather, *Polym. Rev.*, 2009, **49**, 25-63.
51 Y. Ma, X. Cao, X. Feng, Y. Ma and H. Zou, *Polymer*, 2007, **48**, 7455-7460.
52 D.-A. Zha, S. Mei, Z. Wang, H. Li, Z. Shi and Z. Jin, *Carbon*, 2011, **49**, 5166–5172.
53 X. Zhu, Z. Zhang, X. Xu, X. Men, J. Yang, X. Zhou and Q. Xue, *J. Colloid Interface Sci.*, 2012, 367, 443-449.
54 A. Frenot and I. S. Chronakis, *Curr. Opin. Colloid Interface Sci.*, 2003, 8, 64-75.
55 D. Li and Y. Xia, *Adv. Mater.*, 2004, **16**, 1151-1170.
56 W. E. Teo and S. Ramakrishna, *Nanotechnology*, 2006, **17**, R89–R106.
57 A. Greiner and J. H. Wendorff, *Angew. Chem., Int. Ed.*, 2007, **46**, 5670-5703.
58 D. Li, Y. Wang and Y. Xia, *Nano Lett.*, 2003, **3**, 1167.
59 D. Li and Y. Xia, *Nano Lett.*, 2004, **4**, 933.
60 D. Yang, B. Lu, Y. Zhao and X. Jiang, *Adv. Mater.*, 2007, **19**, 3702-3706.
61 M. Bognitzki, W. Czado, T. Frese, A. Schaper, M. Hellwig, M. Steinhart, A. Greiner and J. H. Wendorff, *Adv. Mater.*, 2001, **13**, 70-72.
62 J. M. Deitzel, J. Kleinmeyer, D. Harris and N. C. B. Tan, *Polymer*, 2001, **42**, 261-272.
63 N. K. Adam, The Physics and Chemistry of Surfaces, Oxford University Press, 1930.
64 M. Ma, R. M. Hill, J. L. Lowery, S. V. Fridrikh, G. C. Rutledge, *Langmuir*, 2005, **21**, 5549-5554.
65 A. Singh, L. Steely, H. R. Allcock, *Langmuir*, 2005, **21**, 11604-11607
66 Y. Miyauchi, B. Ding, and S. Shiratori, *Nanotechnology*, 2006, **17**, 5151-5156.
67 Y. Zhu, J. Zhang, Y. Zheng, Z. Huang, L. Feng, L. Jiang, *Adv. Funct. Mater.*, 2006, **16**, 568-574.
68 (a) V. A. Ganesh, A. S. Nair, H. K. Raut, T. M. Walsh and S. Ramakrishna, *RSC Adv.*, 2012, **2**, 2067-2072. (b) V. A. Ganesh, S. S.

Dinachali, A. S. Nair, and S. Ramakrishna, *ACS Appl. Mater. Interfaces*, 2013, **5,** 1527–1532.
69 D. Xu, L. Mammen, H.-J. Butt, and D. Vollmer, *Science*, 2012, **335**, 67-70.
70 L. Xu and J. He, *Langmuir*, 2012, **28**, 7512-7518.
71 S. E. Lee, H.-J. Kim, S.-H. Lee and D.-G. Choi, *Langmuir*, 2013, **29**, 8070-8075.